

Comparison of balloon-carried atmospheric motion sensors with Doppler lidar turbulence measurements

R. G. Harrison,^{a)} A. M. Heath, R. J. Hogan, and G. W. Rogers

Department of Meteorology, University of Reading, P.O. Box 243, Earley Gate, Reading, Berks. RG6 6BB, United Kingdom

(Received 9 December 2008; accepted 2 February 2009; published online 27 February 2009)

Magnetic sensors have been added to a standard weather balloon radiosonde package to detect motion in turbulent air. These measure the terrestrial magnetic field and return data over the standard uhf radio telemetry. Variability in the magnetic sensor data is caused by motion of the instrument package. A series of radiosonde ascents carrying these sensors has been made near a Doppler lidar measuring atmospheric properties. Lidar-retrieved quantities include vertical velocity (w) profile and its standard deviation (σ_w). σ_w determined over 1 h is compared with the radiosonde motion variability at the same heights. Vertical motion in the radiosonde is found to be robustly increased when $\sigma_w > 0.75 \text{ m s}^{-1}$ and is linearly proportional to σ_w . © 2009 American Institute of Physics. [DOI: [10.1063/1.3086432](https://doi.org/10.1063/1.3086432)]

Knowledge on atmospheric motions provides information on convective and turbulent motion, which is relevant to aircraft safety,¹ planetary exploration,² and long recognized to be important for commercial aircraft comfort.³ Standard weather balloons launched for meteorological observations do not record small-scale atmospheric motions, but the addition of a semiconductor magnetic sensor to the instrument package (radiosonde) provides orientation fluctuation information, from which atmospheric motion can be deduced.⁴ A vertically aligned magnetic sensor provides the optimum sensitivity orientation^{5,6} as confirmed by comparing simultaneous data from three orthogonally oriented sensors carried together on several balloon flights.⁷ Beyond qualitatively identifying regions of turbulent motion, calibration of the magnetic data fluctuations to measured atmospheric properties is clearly desirable to show that statistical parameters derived from the package motion data are physically meaningful. An approach for comparing remotely sensed atmospheric properties from a lidar (light detection and ranging) instrument with the *in situ* balloon motion data is described here.

The lower part of the atmosphere (the boundary layer) provides a range of variable turbulent conditions and an upward-facing surface lidar senses atmospheric properties directly above it by the transmission and subsequent detection of an optical pulse. Specifically, a Doppler lidar uses phase information to determine vertical motion associated with the optical reflection, providing frequent profiles of vertical velocity. At Chilbolton Observatory (Hampshire, U.K.), a zenith-pointing Halo-Photonics Doppler lidar (operating wavelength of $1.5 \mu\text{m}$) retrieves vertical velocity data with a height resolution of 36 m every 30 s. While the lidar vertical velocity data are, in principle, suitable for comparison with that from a balloon-carried motion probe at the same heights (Fig. 1), use of the instantaneous (30 s) lidar data for calibration would require the trajectory of the balloon-carried

sensor to remain close to the lidar beam throughout the balloon ascent. As the actual trajectory of the balloon sensor cannot be controlled, beyond arranging the initial release upwind or downwind of the lidar as appropriate, the exact instantaneous comparison is inappropriate. Instead, the lidar data are used to obtain time-averaged profile of atmospheric properties, and these mean atmospheric properties compared with instantaneous data obtained by the balloon sensor at the same heights. The balloon sensor data can therefore be calibrated against the mean atmospheric properties around the time of the launch, which relaxes the need for the trajectory to be immediately adjacent to the lidar beam.

A set of balloon-carried radiosondes with motion sensors has been flown to evaluate this comparison technique with time-averaged Doppler lidar data. Use of many independent balloon flights reduces scatter in the comparison of the data from the different sources, arising from varied trajectories and changes in atmospheric conditions. The radiosondes used for this study were Vaisala RS80 devices suspended 2.5 m beneath a 100 g helium balloon, carrying a data acquisition system⁸ and two magnetic sensors, aligned vertically (Z) and horizontally (X); the Doppler lidar was operated during each balloon flight. The measurement campaign using 12 radiosonde ascents was carried out between 6 March 2007 and 24 July 2007. Air traffic permissions restricted the ascents to a weekly launch time around noon.

Lidar vertical velocity profiles determined for 1 h centered on the launch time were used to calculate a velocity standard deviation profile. Previously,⁷ the radiosondes were programmed to make a short burst of 32 samples from the X and Z sensors in about 9 s, with the values stored in an onboard memory, followed by a slow serial data transmission period lasting for 30 s. For the RS80 radiosonde and 100 g helium balloon combination employed the vertical ascent rate is $\sim 5 \text{ m s}^{-1}$, causing the sampling bursts to be typically separated by about 150 m vertically. Comparison of the lidar and the balloon measurements requires a suitable averaging segment depth h (Fig. 1). If the vertical segment h is too

^{a)}Electronic mail: r.g.harrison@reading.ac.uk.

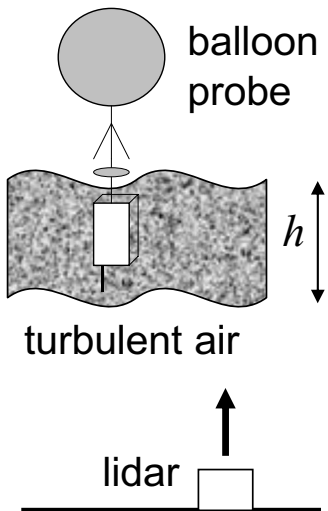


FIG. 1. Concept of the calibration procedure. A balloon-carried motion sensor is launched near to an upward-looking Halo-Photonics Doppler lidar. The lidar is used to determine the vertical velocity w in the air above it. Standard deviations of w (σ_w) are calculated for an hour of data centered on the balloon launch time. Balloon motion data and σ_w are each averaged over the same atmospheric depth segment h . The cuboidal radiosonde package ($95 \times 145 \times 60 \text{ mm}^3$, mass 253 g) has a downward-facing uhf antenna and is attached to the balloon string using a plastic ring. A folded parachute is carried for the descent.

deep, the average will be over the whole depth of the boundary layer, reducing the variability present and therefore requiring more flights; if h is too small, short-lived regions of turbulence sensed by the balloon probes will be time averaged out by the lidar. A compromise of $h=500 \text{ m}$ was found to give several different values per ascent, which used the balloon data effectively. This choice necessarily emphasizes homogenous regions of turbulence, rather than clear air turbulence, which is so variable temporally and spatially that it cannot be sampled reliably by this approach.

Balloon and lidar data obtained and averaged in 500 m vertical segments are analyzed in Fig. 2. Figure 2(a) shows 500 m averaged values of the X and Z balloon magnetometer variability (σ_{Bx} and σ_{Bz} , respectively) for all the balloon flights, with a robust locally weighted regression line added.

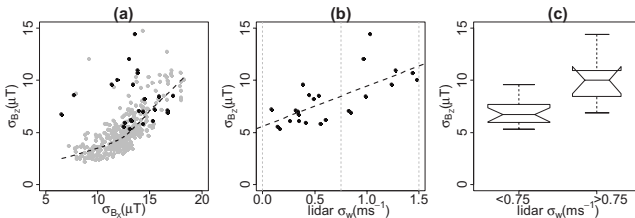


FIG. 2. (a) Standard deviation of magnetic field components in the horizontal (X) and vertical (Z) directions on a balloon-carried radiosonde calculated for 500 m height segments on 12 balloon flights (gray points). The points obtained when the Doppler lidar returns were from below 3 km and with small cloud amounts (cloud fraction less than 0.2) are identified in black with a robust locally weighted regression line added. (b) Hourly-averaged standard deviation of the Doppler lidar vertical velocity (σ_w) plotted against standard deviation of the radiosonde Z -direction magnetometer measurement (σ_{Bz}) for finite data available at the same height. (c) Comparison of the points from (b) divided at $\sigma_w=0.75 \text{ m s}^{-1}$ [regions marked with dotted lines in (b)] with the data represented by notched box plots. (Box plot widths are proportional to the square root of the number of points included; notches on the box plots show 95% confidence levels around the median).

The robust fit line indicates a transition at $\sigma_{Bx} \approx 12 \mu\text{T}$ as found previously,⁷ below which σ_{Bx} and σ_{Bz} are reasonably correlated, but above which they become more scattered. This transition therefore indicates a threshold above which the X and Z motions become increasingly independent. The full set of data cannot be compared directly with the lidar because (1) only some of the values are near to the lidar and (2) some are for nonhomogeneous conditions. Values obtained for comparison with the lidar data have therefore been restricted to the lower atmosphere (height $< 3 \text{ km}$) to prevent the balloon measurements having drifted too far from the lidar. Furthermore, cloudy conditions (cloud fraction > 0.2) have also been excluded, as these present a source of short-term variability unlikely to appear in the time averaging used for the lidar data. The values retained by these criteria are identified in Fig. 2(a). Some of the smaller σ_{Bz} values cluster around the fitted line, but larger σ_{Bz} values are more scattered. Again this indicates that as the amount of motion increases, the X and Z motions become uncorrelated.

Averaged lidar vertical velocity standard deviations (σ_w) and balloon Z motion variability (σ_{Bz}) were examined as histograms, both of which were significantly positively skewed. (95% of the 52 σ_w values were less than 1.26 m s^{-1} .) The subsets of σ_w and σ_{Bz} for lower atmosphere cloud-free points in the same height segments, as identified in Fig. 2(a), are plotted against each other in Fig. 2(b). Preliminary use of a robust locally weighted regression showed that a linear model provided a significant fit to the data, and the linear fit is also shown in Fig. 2(b). The y -intercept is at $\sigma_{Bz}=(5.6 \pm 1.2) \mu\text{T}$, which is effectively the noise level in the Z direction magnetic measurement, at the geomagnetic latitude of the southern U.K. (The sensitivity of σ_{Bz} to σ_w is $(3.85 \pm 1.7) \mu\text{T}/(\text{m s}^{-1})$ and the sensitivity of σ_w to σ_{Bz} is $(0.13 \pm 0.06) (\text{m s}^{-1})/\mu\text{T}$ with uncertainties of two standard errors in each case.) To test the response robustly without assumption of a linear model, the data have been divided at $\sigma_w=0.75 \text{ m s}^{-1}$ and box plots generated for each set of values [Fig. 2(c)]. The box plots show that the Z motion (σ_{Bz}) is significantly greater for $\sigma_w > 0.75 \text{ m s}^{-1}$ than for $\sigma_w < 0.75 \text{ m s}^{-1}$.

Kinetic calibration of the magnetic variability measurements was obtained in a laboratory comparison with an integrated three-axis accelerometer (Analog Devices type ADXL330). This sensing device operates by measuring the deflection of an internal spring-mounted polysilicon micro-machined structure.¹⁰ The ADXL330 accelerometer was fixed inside the standard magnetometer RS80 radiosonde instrument package, aligned along the magnetic sensor X and Z axes. While the instrument package was subjected to steady swinging, the accelerometer outputs were sampled every 0.9 s simultaneously with the magnetic measurements and standard deviations calculated. The Z sensitivity found between the magnetic and accelerometer sensor standard deviations was $(0.012 \pm 0.001) (\text{m s}^{-2})/\mu\text{T}$. Applying this to the balloon, tether length and instrument package described, the relationship between standard deviations in radiosonde vertical acceleration and lidar-derived vertical velocity is $(0.045 \pm 0.02) (\text{m s}^{-2})/(\text{m s}^{-1})$.

Dr. R. Lorenz (Johns Hopkins University) provided helpful comments. This research was funded by the Paul

Instrument Fund of the Royal Society. The 1.5 μm Doppler lidar was acquired with NERC Grant No. NE/C513569/1. Instruments at Chilbolton are operated and maintained by the Rutherford Appleton Laboratory. S. D. Gill assisted with the Civil Aviation Authority arrangements.

¹J. A. Knox, D. W. McCann, and P. D. Williams, *J. Atmos. Sci.* **65**, 3292 (2008).

²R. D. Lorenz, J. C. Zarnecki, M. C. Towner, M. R. Leese, A. J. Ball, B. Hathi, A. Hagermann, and N. A. L. Ghafoor, *Planet. Space Sci.* **55**, 1936 (2007).

³W. H. Pick and G. A. Bull, *Meteorological Office Professional Notes* **6**, 146 (1926).

⁴R. G. Harrison and R. J. Hogan, *J. Atmos. Ocean. Technol.* **23**, 517 (2006).

⁵R. D. Lorenz, *J. Atmos. Ocean. Technol.* **24**, 1519 (2007).

⁶R. G. Harrison and R. J. Hogan, *J. Atmos. Ocean. Technol.* **24**, 1521 (2007).

⁷R. G. Harrison, G. W. Rogers, and R. J. Hogan, *Rev. Sci. Instrum.* **78**, 124501 (2007).

⁸R. G. Harrison, *Rev. Sci. Instrum.* **76**, 026103 (2005).

⁹W. S. Cleveland, *Am. Stat.* **35**, 54 (1981).

¹⁰Analog devices data sheet for ADXL330, www.analog.com.